

# Earthquake Duration and Damping Effects on Input Energy

G. Ghodrati Amiri<sup>1</sup>, G. Abdollahzadeh Darzi<sup>2</sup> and M. Khanzadi<sup>3</sup>

<sup>1</sup>Associate Professor, Email:ghodrati@iust.ac.ir

<sup>2</sup>Ph.D. Candidate

<sup>3</sup>Assistant Professor

Center of Excellence for Fundamental Studies in Structural Engineering,  
College of Civil Engineering, Iran University of Science & Technology,  
Tehran, Iran

**Abstract:** According to performance-based seismic design method by using energy concept, in this paper it is tried to investigate the duration and damping effects on elastic input energy due to strong ground motions. Based on reliable Iranian earthquake records in four types of soils, structures were analyzed and equivalent velocity spectra were computed by using input energy. These spectra were normalized with respect to PGA and were drawn for different durations, damping ratios and soil types and then effects of these parameters were investigated on these spectra. Finally it was concluded that in average for different soil types when the duration of ground motions increases, the input energy to structure increases too. Also it was observed that input energy to structures in soft soils is larger than that for stiff soils and with increasing the stiffness of the earthquake record soil type, the input energy decreases. But damping effect on input energy is not very considerable and input energy to structure with damping ratio about 5% has the minimum value.

**Keywords:** PGA; duration of strong ground motion; damping ratio; input energy spectrum.

## 1. Introduction

Design of structures with performance-based design especially based on energy is one of the methods noticed by researches in the recent years [1-8]. Unlike present methods which are based on peak accelerations that ignore duration and hysteretic behavior effects on structural design, design based on energy not only considers the effects of these parameters, but also it can describe treatment of structures during an earthquake, better than present methods.

In this method formed on the basis of energy concepts and energy balance equation, energy criterion expresses that the structure collapses when the amount of capacity energy lower than the demand energy to dissipate through inelastic deformations is exerted.

Researches considered that among various types of energy the input energy,  $E_I$  which is a very stable parameter of structural response, is suitable for energy-based design. Input energy is a measure of energy that earthquake inputs to structures during the ground motion. Based on definition, two types of input energy exist [9], relative input energy,  $E_I$  and absolute input energy,  $E'_I$ . The difference between  $E_I$  and  $E'_I$  is the effect of the rigid body translation of structure. If  $E_I$  and  $E'_I$  are evaluated at the end of ground motion duration, it can be considered that they differ in the very short and very long period ranges only.

In a structure if its supply energy was larger than its imposed energy, all the energy exerted to the structure during ground motion is dissipated through damping and hysteretic cyclic behavior of structure at the end of

ground motion. This inelastic cyclic behavior causes partial damages in structures and with accumulation of these partial damages, structures collapse. Therefore the input energy demand can be assumed as a reliable tool to predict the seismic hazard and seismic design.

Thus evaluation of influence of structural parameters, characteristics of earthquake records and soil conditions on input energy are important.

In this paper, the effects of ground motion duration, structural damping and soil type on input energy were studied, by use of 110 Iranian earthquake records. Because these records are collected from different earthquakes with various *PGA*'s, in order that the effects of earthquake *PGA* in result of each analysis are vanished, and also their responses can be added together, the amount of input energy was divided by its *PGA* and the spectrum curve of input energy was drawn. This procedure is also performed in the previous researches on this topic such as Benavent–Climent's work [2].

## 2. Literature Review

Previously many of researches investigated the duration of ground motion, damping of structure and soil condition influences on input energy and obtained different conclusions.

Zahrah and Hall [11] computed the input energy for eight earthquake records and they considered that ductility, damping and past-to-pre yield stiffness ratios have small effects on the input and hysteretic energies for a structure with bilinear behavior.

Based on many analyses, McKevitt et al.

[12], Akiyama [13] and Nakashima et al. [14] observed that damping does not have a significant influence on the earthquake input energy.

Results of the study by Bruneau and Wang [15] indicated that damping ratios smaller than 5% have a minor influence on the input energy.

Rahnama and Manuel [16] computed the input energy for ductility ratios of 2 and 6 with 5% damping for six sets of 19 accelerations each, actual records and simulated records with the same duration 5, 10, 15 and 20 s. They considered that when duration increases, the input energy increases.

Khashaee et al. [17] computed the relative input energy for 10 accelerations with short duration (shorter than 8 s) and 10 with long duration (longer than 18 s) of strong ground motions. They observed that as the duration of strong ground motions increases, the input energy also increases. They computed the relative input energy for structures with damping ratios 0, 2, 5, 10, 20 and 40% for three accelerations with short duration and three with long duration of strong ground motion. They observed that for damping ratios smaller than 5%, damping has little influence on the input energy while for damping ratios greater than 5%, damping has a significant influence on the input energy spectra, particularly for very long natural periods as the damping increases, the input energy increases.

## 3. Theoretical Background

When a viscous damped single mass elastic oscillatory system, *SDOF*, vibrates subject to a unidirectional horizontal ground motion, its equilibrium equation can be expressed as follows [9].

$$M\ddot{y}_i + C\dot{y} + Ky = 0 \quad (1)$$

Where  $M$ ,  $C$ ,  $K$  and  $y$  are mass, viscous damping coefficient, spring constant and relative displacement of the mass, respectively.  $y_t = y + x_g$  is absolute (or total) displacement of the mass.  $\dot{y}$  and  $\ddot{y}_t$  are first derivation of  $y$  and the second derivation of  $y_t$  with respect to time respectively.  $x_g$  and  $\ddot{x}_g$  are earthquake ground displacement and ground acceleration, respectively.

By letting  $\ddot{y}_t = \ddot{y} + \ddot{x}_g$  Equation (1) can be re-written as follows:

$$M\ddot{y} + C\dot{y} + Ky = -M\ddot{x}_g \quad (2)$$

Where,  $\ddot{y}$  is the second derivation of  $y$  with respect to time.

Therefore the structural system in a moving base system can be treated conveniently as an equivalent system with a fixed base subjected to an effective horizontal dynamic force of magnitude  $-M\ddot{x}_g$ . Depending upon whether Equation (1) or (2) is used to derive the energy equation, different definitions of input energy may result.

#### Method 1- Derivation of absolute energy equation

If both sides of Equation (1) are multiplied by  $dy (= \dot{y}dt)$  and then integrated over the entire duration of an earthquake,  $t_0$ , Equation (1) reduces to the following energy balance equation:

$$\int_0^{t_0} M\ddot{y}_t (\dot{y}dt) + \int_0^{t_0} C\dot{y}(\dot{y}dt) + \int_0^{t_0} Ky(\dot{y}dt) = 0 \quad (3)$$

Replacing  $\dot{y}$  by  $\dot{y}_t - \dot{x}_g$  in the first term of Equation (3), then

$$\int_0^{t_0} M\ddot{y}_t (\dot{y}_t - \dot{x}_g)dt + \int_0^{t_0} C\dot{y}^2 dt + \int_0^{t_0} Ky\dot{y}dt = 0 \quad (4)$$

$$\int_0^{t_0} M\ddot{y}_t \dot{y}_t dt + \int_0^{t_0} C\dot{y}^2 dt + \int_0^{t_0} Ky\dot{y}dt = \int_0^{t_0} M\ddot{y}_t \dot{x}_g dt \quad (5)$$

$$\frac{1}{2}M\dot{y}_t^2 + \int_0^{t_0} C\dot{y}^2 dt + \frac{1}{2}Ky^2 = M \int_0^{t_0} \ddot{y}_t \dot{x}_g dt$$

$$E'_k + E_d + E_s = E'_I \quad (6)$$

Where:

$$E'_k = \frac{1}{2}M\dot{y}_t^2 \quad , \quad E_d = \int_0^{t_0} C\dot{y}^2 dt$$

$$E_s = \frac{1}{2}Ky^2 \quad , \quad E'_I = M \int_0^{t_0} \ddot{y}_t \dot{x}_g dt$$

Here  $E'_k$ ,  $E_d$  and  $E_s$  are absolute kinetic energy, the energy dissipated by damping mechanism and the energy absorbed by spring, respectively, and  $E'_I$  is defined as the absolute input energy. This definition is physically meaningful in where the term  $M\dot{y}_t$  represents the inertia force applied to the structure. This force, from Equation (1), is equal to restoring force plus damping force, which is the same as the total force applied to the structure foundation. Therefore  $E'_I$  represents the work done by the total base shear at the foundation through the foundation displacement.

#### Method 2 – Derivation of relative energy equation

If both sides of Equation (2) are multiplied by  $dy (= \dot{y}dt)$  and then integrated over the entire duration of an earthquake,  $t_0$ , Equation (2) reduces to the following energy balance equation:

$$\int_0^{t_0} M\ddot{y}(\dot{y}dt) + \int_0^{t_0} C\dot{y}(\dot{y}dt) + \int_0^{t_0} Ky(\dot{y}dt) = \int_0^{t_0} -M\ddot{x}_g(\dot{y}dt) \quad (7)$$

$$\int_0^{t_0} M\ddot{y}\dot{y}dt + \int_0^{t_0} C\dot{y}^2 dt + \int_0^{t_0} Ky\dot{y}dt = \int_0^{t_0} -M\ddot{x}_g\dot{y}dt \quad (8)$$

$$\frac{1}{2}M\dot{y}^2 + \int_0^{t_0} C\dot{y}^2 dt + \frac{1}{2}Ky^2 = -M \int_0^{t_0} \ddot{x}_g \dot{y}dt \quad (9)$$

$$E_k + E_d + E_s = E_I \quad (10)$$

Where:

$$E_k = \frac{1}{2} M \dot{y}^2 \quad , \quad E_d = \int_0^{t_0} C \dot{y}^2 dt$$

$$E_s = \frac{1}{2} K y^2 \quad , \quad E_I = -M \int_0^{t_0} \ddot{x}_g \dot{y} dt$$

Here  $E_k$  is relative kinetic energy and  $E_I$  is defined as relative input energy. This definition of input energy physically represents the work done by the static equivalent lateral force ( $-M \ddot{x}_g$ ) on the equivalent fixed-base system.

#### Evaluation of the difference between input energies from different definitions

The difference between the input energies of Methods 1 and 2 is derived below:

$$\begin{aligned} E'_I &= M \int_0^{t_0} \ddot{y}_t \dot{x}_g dt = M \int_0^{t_0} \ddot{y}_t (\dot{y}_t - \dot{y}) dt \\ &= M \int_0^{t_0} \ddot{y}_t \dot{y}_t dt - M \int_0^{t_0} \ddot{y}_t \dot{y} dt \\ &= M \int_0^{t_0} \ddot{y}_t \dot{y}_t dt - M \int_0^{t_0} (\ddot{y} + \ddot{x}_g) \dot{y} dt \\ &= \frac{1}{2} M \dot{y}_t^2 - \int_0^{t_0} \dot{y} \ddot{y} dt - \int_0^{t_0} \dot{y} \ddot{x}_g dt \\ &= \frac{1}{2} M \dot{x}_g^2 + M \dot{x}_g \dot{y} + E_I \\ &= \frac{1}{2} M (\dot{y} + \dot{x}_g)^2 - \frac{1}{2} M \dot{y}^2 + E_I \\ &= \frac{1}{2} M (\dot{y}^2 + \dot{x}_g^2 + 2\dot{x}_g \dot{y}) - \frac{1}{2} M \dot{y}^2 + E_I \\ E'_I - E_I &= \frac{1}{2} M (\dot{x}_g^2 + 2\dot{x}_g \dot{y}) \end{aligned} \quad (11)$$

The values of  $E_I$  and  $E'_I$  for very long and very short period structures can be calculated. For a structure with a very long period ( $T \rightarrow \infty$ ), the input energy tends to converge to a constant value, depending upon which definition of input energy is used. For a structure with an infinitely long period,

$$y = -x_g \text{ and } y_t = y + x_g = 0,$$

$$\text{therefore } E'_I = 0 \text{ and } E_I = 0.5 M \dot{x}_g^2$$

i.e. the difference between the input energies and for a structure with a very long period is equal to  $0.5 M \dot{x}_g^2$ . If the input energy  $E_I$  is evaluated at the end of duration, its value will be very small because  $\dot{x}_g$  tends to be vanishingly small. If  $E_I$  is evaluated as the maximum throughout the duration, then  $E_I$  will then converge to  $0.5 M \dot{x}_{g(max)}^2$  for long period structures.

For a structure with very short period ( $T \rightarrow 0$ ), the input energy will also converge to a constant value, depending upon the definition used. For a structure with zero period, i.e. a rigid structure,

$$\ddot{y}_t = \ddot{x}_g \text{ and } y_t = x_g,$$

$$\text{therefore } E'_I = 0.5 M \dot{x}_g^2 \text{ and } E_I = 0$$

i.e. the maximum difference between the input energies spectra for a structure with zero period is equal to  $0.5 M \dot{x}_{g(max)}^2$ .

Although absolute input energy might be physically more meaningful but relative input energy is considered more significant for the purpose of seismic design [10]. This research has adopted the relative expression of input energy.

Akiyama [13] expressed  $E_I$  in terms of equivalent pseudo-velocity,  $V_E$ , which is defined as follows:

$$V_E = \sqrt{2E_I / M} \quad (12)$$

Also, for a given earthquake record, he defined a relationship between the total input energy,  $E_I$ , expressed in terms of the equivalent pseudo-velocity by  $V_E$  equation

(12), and the natural period of system,  $T$ , as input energy spectrum,  $V_E$  versus  $T$ .

In this research in order to obtain and normalize the input energy spectrum, following steps are performed:

1. For each ground motion acceleration record available in the region, the relative input energy spectrum  $V_E$  versus  $T$  corresponding to an elastic SDOF system is obtained. In calculating  $V_E$ , Akiyama [13] showed that the contributions of the rotational and vertical components of the quake are in general negligible, and can be estimated from the two horizontal components as follows:

$$V_E = \sqrt{V_{E,NS}^2 + V_{E,EW}^2} \quad (13)$$

Where  $V_{E,NS}$  and  $V_{E,EW}$  represent the energy input by the north-south (NS) and east-west (EW) components, respectively.

2. For each ground motion record, similar to the previous step, the peak ground accelerations ( $PGA$ ) at any instant of time can be determined from its horizontal components as follows [2]:

$$\ddot{X}_{g,t} = \sqrt{\ddot{X}_{g,t,NS}^2 + \ddot{X}_{g,t,EW}^2} \quad (14)$$

$$PGA = \text{Max}(\ddot{X}_{g,t})$$

Where  $\ddot{X}_g$  is ground accelerations  $\ddot{X}_{g,t,NS}$  and  $\ddot{X}_{g,t,EW}$  are the north- south and east-west components of  $\ddot{X}_g$ , respectively.

3. Because different records are collected from different earthquakes with various  $PGA$  and in order that the earthquake  $PGA$  effects in response of each analyses are vanished and these responses can be added together, for each record, the amount of  $V_E$  (computed in the first step) is divided by its  $PGA$  (computed in the second step) and

consequently  $f = V_E / PGA$  for each record is computed and spectrum curve of  $f$  versus  $T$  was drawn.

#### 4. Selection of Earthquake Records

Similar to many other researches, as the first step of this study, a suitable selection of earthquake records was needed. For this purpose Iranian earthquake records were chosen.

Iran is among the countries located in high seismicity regions (Alpine-Himalaya seismic belt) and is very often subjected to relatively strong ground motions resulting in huge losses of lives and costly damages due to occurrence of numerous destructive earthquakes. In recent history, this country has had many destructive strong ground motions e.g. Naghan, Tabas, Manjil earthquakes and more recently Bam earthquake in December 26, 2003 which killed more than 40000 and injured around 25000 people in Bam city [19].

The earthquake records of Iran are unique in terms of characteristics such as focal depth, fault mechanism, soil type, etc. and their number in comparison with those used in similar researches which can make the results of this study very useful for researchers in this field. Since the authors had a relatively complete knowledge of Iranian earthquake databases and the related necessary information (availability of data regarding the causative earthquakes, the possibility of proper correction of the records and geological information about the earthquake recording stations), 110 records were selected. After a comparative study of the different researches that have been performed in Iran in the past [20 – 23], the ground types on which recording machines

were located were classified according to the soil conditions defined by Iranian Earthquake Code of Practice, Standard No. 2800 [24], which is based on the geological characteristics and the shear wave velocity [25-26]. In this code soils are divided in 4 types, based on shear wave velocity,  $V_S$ . These groups are ground type 1 with  $V_S > 750$  m/s, ground type 2 with  $375 \text{ m/s} < V_S < 750$  m/s, ground type 3 with  $175 \text{ m/s} < V_S < 375$  m/s and ground type 4 with  $V_S < 175$  m/s that can be named bed rock, stiff soil, medium soil and soft soil, respectively. By this definition 110 records used in this research were divided in 30, 27, 39 and 14 records for ground types 1, 2, 3 and 4, respectively. The minimum and maximum earthquake durations for these records are (1.25s, 34.76s), (0.35s, 20.48s), (0.77s, 38.66s) and (4.5s, 30.11s) in four ground types, respectively (Tables 1 to 4). It should be noted that in all following tables the parameter, effective duration, is duration base-intensity that by definition is the time between 5% and 95% of the total energy induced by result of two horizontal components of earthquake [18]. In these tables  $PGA_{NS}$  and  $PGA_{EW}$  are the maximum values of the north- south and east-west components of ground accelerations, respectively.

## 5. Input Energy Spectra

For each ground type, the pseudo-velocity response spectrum,  $V_E$  versus  $T$ , corresponding to an elastic *SDOF* system was obtained by calculating the pseudo-velocity components (i.e.  $V_{E,NS}$  and  $V_{E,EW}$ ) and then these were divided to  $PGA$  for each ground motion record.

In the first step and for investigating duration effects on input energy, since there is a time

gap in the effective durations of these records, based on the number of records and parametric study on the differences of their results in each soil types, these records were divided into two groups in terms of effective durations. Only ground type 3 was divided in three groups. For each set, based on Akiyama recommendations [13], the normalized pseudo-velocity response spectrum was calculated for elastic *SDOF* system with 10% damping ratio (Figure 1 to 4). Then for determining relation between duration and input energy, energies imposed to structures with natural periods 0.2 and 1 second in ground type 1 affected by earthquake with different duration were computed and they were indicated in Figure 5. In part c of Figure 5 relation between earthquake duration and mean of energy inputted to structures with different natural periods between 0.1 to 3 second was shown. Finally for each set of durations the mean value of these spectral curves was calculated (Figure 6).

In the second step and for accessing damping ratios effects on input energy, these spectra were calculated and were drawn for elastic *SDOF* system with damping ratios  $\zeta = 1, 3, 5, 7, 10, 15$  and 20% affected by earthquakes with different durations (Figure 7), and then the mean value of these spectral curves were calculated and were shown in Figure 8.

Finally for indicating the soil condition effects on input energy, the mean normalized pseudo-velocity response spectra corresponding to elastic *SDOF* system with 10% damping ratio was obtained, and drawn in Figure 9 for different ground types with different records and various durations.

## 6. Results and Discussions

### 6.1- Duration effects on input energy

Figures 1, 2 and 4 indicate normalized

**Table 1** Characteristics of selected records for ground type 1

Record no	Station name	Duration(s)	Effective Duration(s)	Year	Epicentral distance(km)	Acceleration(cm/s <sup>2</sup> )		
						PGA <sub>NS</sub>	PGA <sub>EW</sub>	PGA
1043	GHAEN	19.57	10.48	76	10	133.95	148.99	170.13
1049-2	SEYEHCHESHMEH	11.61	7.25	76	4	14.63	16.66	23.15
1054-1	NAGHAN	21.33	3.11	77	5	707.82	543.91	740.99
1082-1	DEYHUK	58.40	34.76	78	37	317.96	374.43	442.70
1084-1	TABAS	48.99	18.98	78	27	805.97	809.93	820.62
1084-18	TABAS	15.13	4.15	78	27	44.83	87.07	99.80
1084-19	TABAS	19.47	7.97	78	26	61.10	47.14	63.11
1084-21	TABAS	12.40	1.20	78	21	123.06	106.27	161.30
1084-34	TABAS	19.06	3.36	78	22	121.63	112.49	214.10
1084-46	TABAS	16.22	6.08	78	17	97.09	61.79	97.23
1084-47	TABAS	15.28	2.56	78	64	141.64	115.65	149.46
1084-48	TABAS	15.28	2.72	78	64	140.19	137.16	174.92
1347-4	SIRCH	18.63	5.76	89	38	66.38	51.68	73.33
1362-1	ABBAR	58.17	35.08	90	43	385.22	436.63	505.99
1419-1	SEFIDRUD DAM	25.19	5.30	91	15	322.90	277.89	327.30
1425	SIRCH	7.67	2.25	92	8	50.22	87.22	88.16
1492-15	ZARRAT	25.61	6.57	94	21	99.22	81.37	119.30
1492-16	ZARRAT	43.53	7.12	94	26	310.81	230.33	311.30
1492-2	ZARRAT	17.93	8.22	94	34	21.78	21.14	26.66
1492-6	ZARRAT	33.29	6.80	94	15	190.76	231.42	300.91
1494-2	KAVAR	17.93	8.60	94	32	18.16	13.89	24.56
1495	MOHARLO	17.93	8.60	94	46	18.16	13.89	24.56
1519-4	ZARRAT	20.49	5.91	94	29	65.82	53.99	70.16
1537	SEFIDRUD DAM	17.93	9.12	95	33	18.16	6.56	24.47
1547-2	SEFIDRUD DAM	20.49	5.24	95	35	65.05	16.45	66.36
1551-2	SHABESTAR	17.93	4.94	95	12	38.75	40.40	47.64
1562-2	ZARRAT	15.37	6.00	95	32	27.55	14.87	31.76
1583-3	SAADABAD	34.57	14.26	96	12	49.18	45.20	75.11
1589-1	SAADABAD	29.45	9.85	96	12	43.84	47.76	52.18
1589-3	SAADABAD	25.61	4.02	96	12	51.75	95.09	107.54

**Table 2** Characteristics of selected records for ground type 2

Record no	Station name	Duration(s)	Effective Duration(s)	Year	Epicentral distance(km)	Acceleration(cm/s <sup>2</sup> )		
						PGA <sub>NS</sub>	PGA <sub>EW</sub>	PGA
1006-1	BANDARABBAS	30.01	12.14	75	36	84.40	119.92	127.4
1022-2	PARSABAD	26.68	5.28	76	53	89.16	142.23	156.0
1044	KHEZRI	21.05	13.66	76	46	25.81	18.91	26.6
1046-1	MAKU	28.10	18.68	76	53	76.34	64.81	92.4
1047-6	VANDIK	2.01	0.35	76	11	226.65	155.79	373.9
1050-1	BANDARABBAS	45.24	20.48	77	48	86.79	140.36	155.7
1050-2	BANDARABBAS	21.35	15.74	77	53	26.52	39.96	43.3
1050-3	BANDARABBAS	17.51	11.24	77	58	25.76	40.45	44.0
1050-4	BANDARABBAS	30.85	19.19	77	43	43.41	37.80	43.5
1113	KHAF	32.45	14.73	79	103	71.05	67.57	75.5
1322-2	KAZERUN	18.18	11.97	88	37	32.64	32.52	38.3
1360	MANJIL	11.05	1.79	90	16	394.76	364.45	472.0
1377-1	MANJIL	9.59	3.32	90	21	125.10	146.54	237.5
1377-2	MANJIL	9.90	3.23	90	42	101.30	50.75	101.7
1397-3	MANJIL	14.43	3.43	90	37	47.83	104.19	104.4
1490-2	MEMAND	27.17	6.12	94	17	415.69	417.56	483.9
1490-6	MEMAND	10.69	8.52	94	23	169.10	173.69	181.6
1497	FARSABAD	26.89	18.22	94	54	12.42	22.81	22.9
1498	BABANAR	24.33	13.78	94	51	28.67	39.03	39.0
1500-4	ZANJIRAN	21.77	5.69	94	17	60.95	71.10	92.4
1502-4	ZANJIRAN	21.77	3.14	94	66	200.99	194.20	271.6
1502-8	ZANJIRAN	24.33	6.83	94	12	78.35	92.32	121.7
1502-9	ZANJIRAN	64.01	5.54	94	12	868.12	1140.30	1158.6
1507	DEZ DAM	17.93	6.67	94	31	23.16	25.50	33.1
1508-2	ANDIMESHK	20.49	9.04	94	40	18.16	35.99	36.0
1532	DEHBALA	19.21	8.22	95	32	31.30	25.13	39.1
1539	MASHHAD	16.65	9.34	95	74	19.15	14.10	20.4

**Table 3** Characteristics of selected records for ground type 3

Record no	Station name	Duration(s)	Effective Duration(s)	Year	Epicentral distance(km)	Acceleration( $\text{cm/s}^2$ )		
						$\text{PGA}_{\text{NS}}$	$\text{PGA}_{\text{EW}}$	PGA
1042	SEDEH	18.41	8.87	76	56	12.73	25.82	27.74
1048-1	KALAT	19.92	9.57	76	9	27.56	32.73	44.42
1070	KONARTAKHTEH	15.76	12.84	77	7	32.18	28.54	49.97
1102	BAJESTAN	12.01	8.28	79	145	38.74	27.72	45.67
1117	SEDEH	37.16	24.36	79	85	27.81	23.45	34.61
1131	TORBATEHYDAREYH	44.84	24.98	79	143	43.73	37.67	47.55
1138-1	SEDEH	49.53	21.85	79	87	85.86	76.17	87.54
1173	RAFSANJAN	37.63	22.95	81	178	46.96	39.92	57.09
1176-15	GOLBAFT	13.49	7.90	81	30	42.72	24.09	44.96
1176-22	GOLBAFT	6.01	2.23	81		23.27	53.73	58.50
1176-5	GOLBAFT	59.33	38.66	81	13	208.42	274.68	293.90
1177	ZARAND	43.93	31.11	81	48	40.99	40.05	50.00
1178-2	RAVAR	14.47	10.95	81	169	65.54	50.69	74.74
1183-1	GOLBAFT	13.87	4.72	81	17	94.69	57.88	104.63
1183-10	GOLBAFT	17.07	3.27	81	6	94.60	161.88	186.77
1224-2	ARDEL	15.99	9.76	84	15	161.77	188.70	227.00
1258-2	FIRUZABAD	20.41	4.72	85	48	93.52	60.72	125.45
1329	NURABADMAMASANI	17.31	10.44	88	24	51.29	70.16	87.17
1341-1	ARDEL	20.00	9.82	89	14	154.00	92.30	154.30
1368-1	RUDBAR1	4.26	1.50	90	48	73.52	95.61	107.36
1372	ESHTEHARD	45.87	24.32	90	144	68.94	54.10	77.98
1382-6	RUDBAR1	11.01	2.68	90	43	305.28	161.45	334.15
1382-7	RUDBAR1	13.39	5.16	90	36	182.73	92.10	188.02
1395-1	RUDBAR1	5.01	0.77	90	52	47.49	94.67	98.08
1420-4	RUDBAR1	19.99	6.75	91	12	245.07	245.07	417.39
1420-6	RUDBAR1	12.58	1.58	91	35	124.59	86.88	155.94
1486-1	FIRUZABAD	28.17	9.81	94	29	128.68	68.27	131.20
1489-1	FIRUZABAD	13.01	7.59	94	25	61.71	59.87	73.15
1493-2	FIRUZABAD	38.41	8.89	94	15	194.01	157.34	280.25
1512-1	SEDEH	18.81	5.45	93	46	33.27	42.54	43.48
1518-2	FIRUZABAD	15.37	9.08	94		9.75	7.95	12.74
1528-16	FIN	15.37	11.42	95	48	19.41	21.63	26.07
1528-3	FIN	32.01	3.26	95	26	476.32	440.08	657.59
1529-3	LALY	21.77	10.82	95	41	25.87	24.03	34.53
1530-1	NIR	21.77	5.77	94		81.75	46.47	81.86
1535-2	RUDBAR1	17.93	2.61	95	30	97.80	92.89	113.60
1541	RASHT5	15.37	9.67	95	32	16.97	23.53	25.58
1550-1	MASAL	15.37	5.84	94	34	6.56	7.53	9.47
1575-1	BABAKALAN	15.37	5.35	95	38	23.84	20.34	24.86

**Table 4** Characteristics of selected records for ground type 4

Record no	Station name	Duration(s)	Effective Duration(s)	Year	Epicentral distance(km)	Acceleration( $\text{cm/s}^2$ )		
						$\text{PGA}_{\text{NS}}$	$\text{PGA}_{\text{EW}}$	PGA
1007	MINAB	28.48	19.10	75	73	28.33	22.70	30.78
1013	TONEKABON	14.36	7.27	75	34	32.27	17.50	45.54
1150	LAHIJAN	13.69	8.71	80	33	56.57	98.46	104.98
1168	KERMAN	19.95	16.26	81	75	41.14	31.79	41.16
1174	KERMAN	38.08	21.23	81	75	99.11	84.47	106.52
1185	RUDSAR	19.02	8.09	80	16	111.97	66.97	112.97
1355	RUDSAR	53.13	28.69	90	90	84.81	78.55	100.89
1357-1	LAHIJAN	60.55	30.11	90	76	104.56	167.25	185.69
1359	TONEKABON	35.99	25.06	90	131	106.52	64.56	129.67
1369	ROODSHOR	18.13	14.10	90	198	38.05	43.18	48.16
1506-5	HOSSEINEHOLYA	15.37	6.91	94	31	21.65	18.56	27.47
1506-8	HOSSEINEHOLYA	15.37	4.50	94		22.96	34.70	41.29
1571-10	SHABANKAREH	43.53	17.24	96	13	49.43	85.61	88.88
1585-1	SHABANKAREH	26.89	5.72	96	17	47.29	102.86	103.53



pseudo-velocity spectra ( $f$ ) in different ground types imposed by two sets of duration: short duration and long duration records. In Figure 3 these sets were converted to three sets of duration (short, medium and long durations). In all of these figures in set with longer duration, the average of normalized pseudo-velocity spectra ( $f$ ) obviously is bigger than  $f$  in those of set with short duration. These figures show that the predominate periods of 4 ground types are different. These periods depend on various parameters, mostly on the frequency content of earthquake which is filtered by site soil. Figure 5 in parts a and b shows values  $f$  versus duration for natural periods 0.2 and 1 second and also in part c shows mean values  $f$  versus duration for all natural periods of 0.1 to 3 seconds. All parts of this figure show that with increasing in duration the value of input energy (or  $f$ ) doesn't increase necessarily and variation of  $f$  is very irregular.

Different parts of Figure 6 show the mean value of  $f$  calculated for each set of durations in each ground types. This figure shows that although value of  $f$  does not exactly increase with increase in duration, the average of these values does increase and it obviously indicates that the mean value of  $f$  in long duration is about 2 to 3 times bigger than of the mean value of  $f$  in short duration. It means that input energy in long duration is about 4 to 9 times bigger than input energy in short duration. These results approve the results that were concluded by Rahnama and Manuel [16] and Khashaee et al. [17].

### 6.2- Damping effects on input energy

Figure 7 shows damping effects on input energy. This figure indicates that in all ground types damping effects on spectral normalized pseudo-velocity (or input energy) is small and with increase in damping ratios  $f$  remains almost constant, during each natural

period. Figure 8 that is drawn for mean  $f$  versus damping ratios for different natural periods approves this result more clearly. Figure 8 shows the influence of damping ratios on input energy. This figure drawn for all natural periods, indicates that in all of ground types an increase in damping ratios will result in  $f$  (or input energy) to decrease for small damping ratios ( $\zeta \leq 5\%$ ) and increase for large damping ratios ( $\zeta > 5\%$ ). In the other words, the amount of  $f$  for a damping ratio of  $\zeta = 5\%$  is minimum. Of course under both conditions (small and large damping ratios), the variation of  $f$  is not fast. These results approve the results concluded by Bruneau and Wang [15] and Khashaee et al. [17].

### 6.3- Ground type effects on input energy

Figure 9 shows mean spectral input energy of ground motions recorded in four ground types for structures with a damping ratio of 10% and with different natural periods of 0.1 to 3 seconds. All of the previous figures and also Figure 9 obviously indicate that input energy decreases with increasing in stiffness of soil. Figure 9 shows that in very short natural periods ( $T \leq 0.2$  s) the amount of  $f$  for all ground types is equal but in longer natural periods ( $T > 0.2$ s) the amount of  $f$  (or input energy) increases with decreasing in stiffness in soil where earthquake record is registered.

## 7. Summary of Results

The main objective of this paper is to assess the effects of duration, damping ratios and ground type on elastic input energy in *SDOF* systems. Using Iranian earthquake records, first 110 earthquake records were selected and divided in four ground types based on categorization criteria defined in Iranian seismic code of practice [24]. Then the input

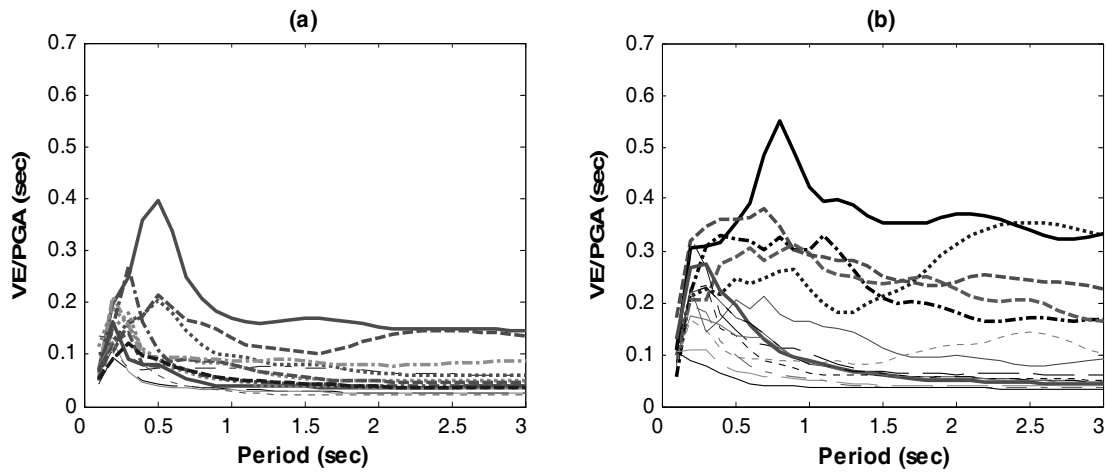


**Fig.1** Input energy spectra of the ground motions recorded in ground type 1  
(a) for duration  $\leq 6$  sec (b) for duration  $> 6$  sec

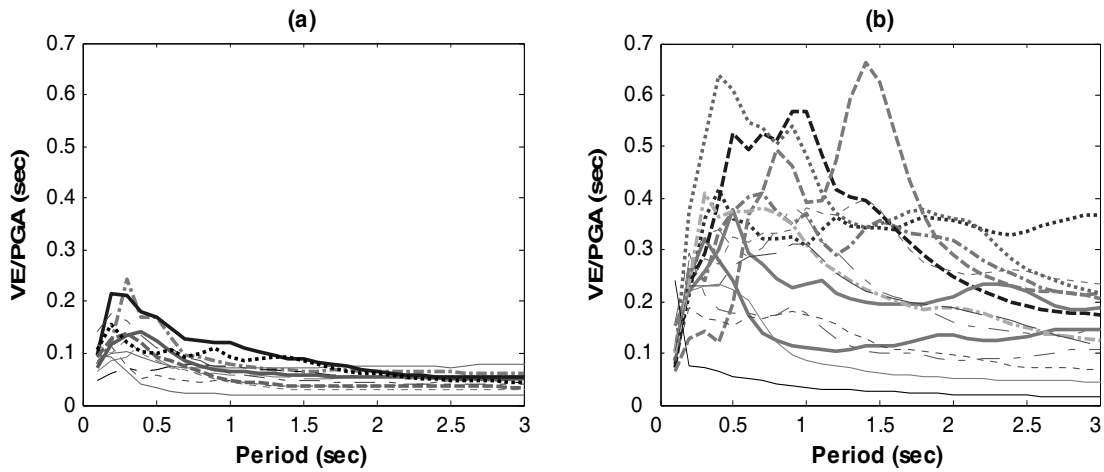


**Fig.2** Input energy spectra of the ground motions recorded in ground type 2  
(a) for duration  $\leq 8$  sec (b) for duration  $> 8$  sec

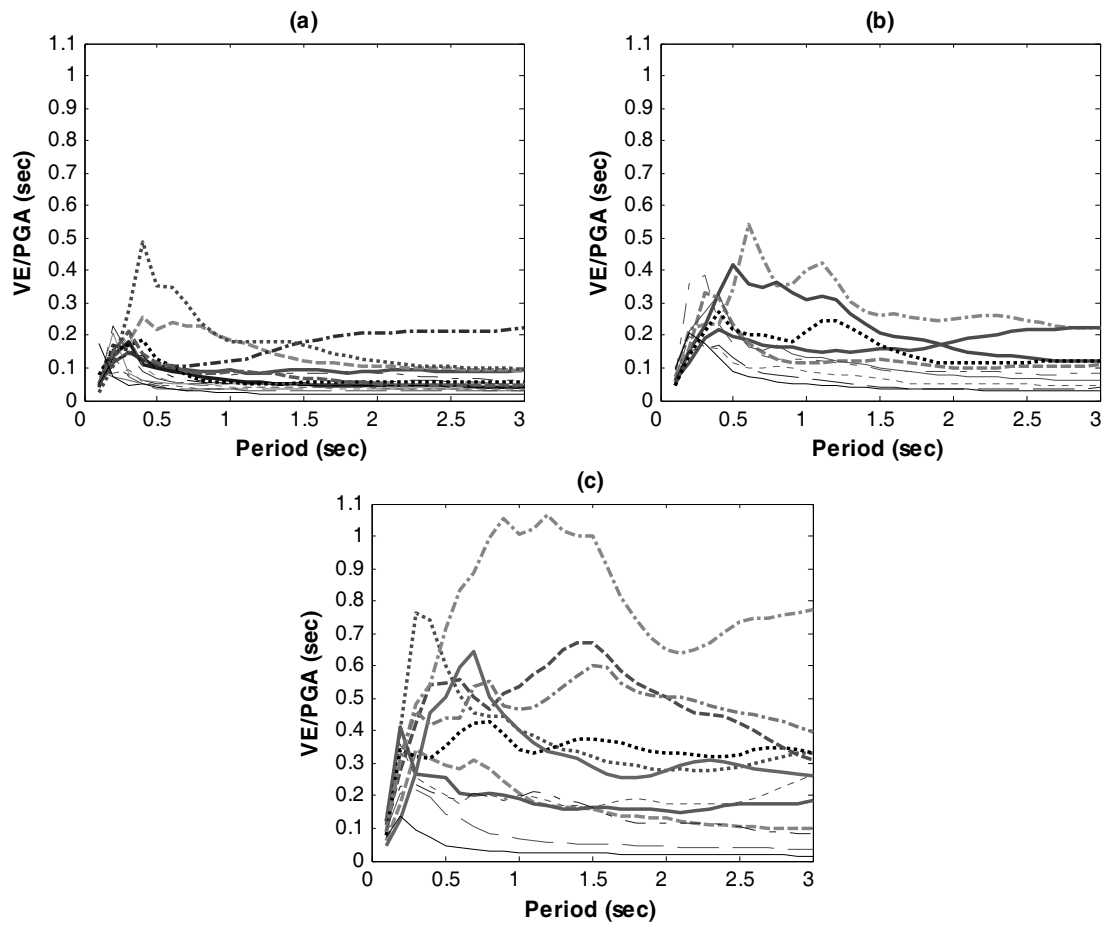


**Fig.3** Input energy spectra of the ground motions recorded in ground type 3  
 (a) for duration = 7 sec (b) for 7 sec <= duration <= 10 sec (c) for duration > 10 sec

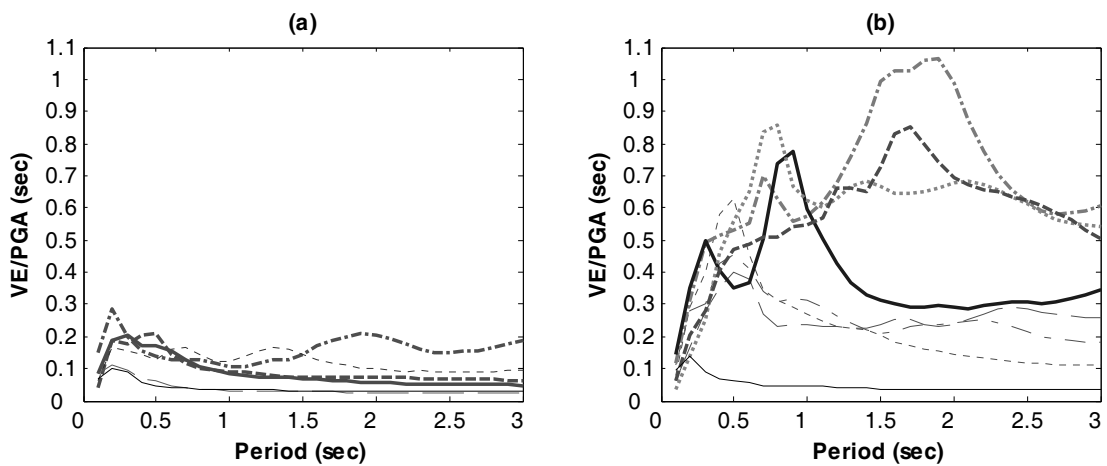


**Fig.4** Input energy spectra of the ground motions recorded in ground type 4  
 (a) for duration <= 10 sec (b) for duration > 10 sec

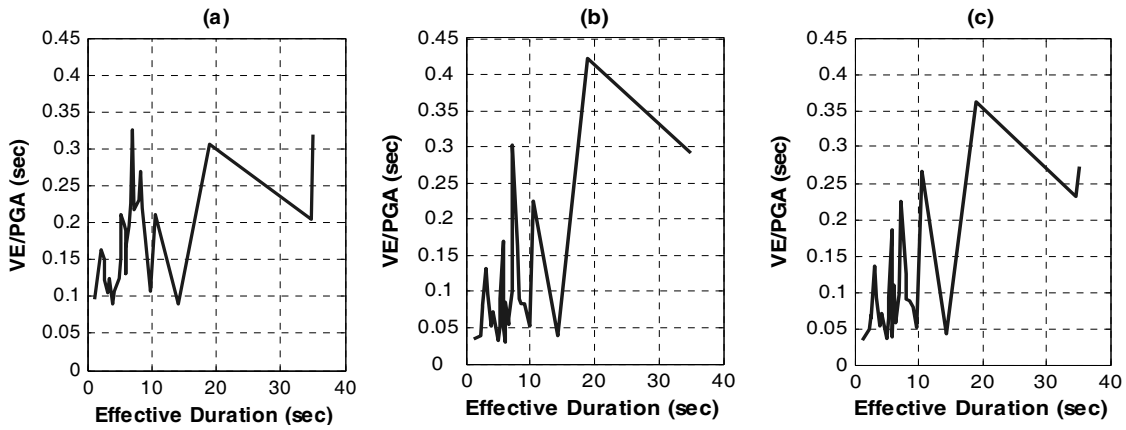


**Fig.5** Spectral input energy versus duration of the ground motions recorded in ground type 1  
 (a) for  $T=0.2$  sec (b) for  $T=1$  sec (c) mean  $f$  for all  $T$  between 0.1 sec to 3 sec

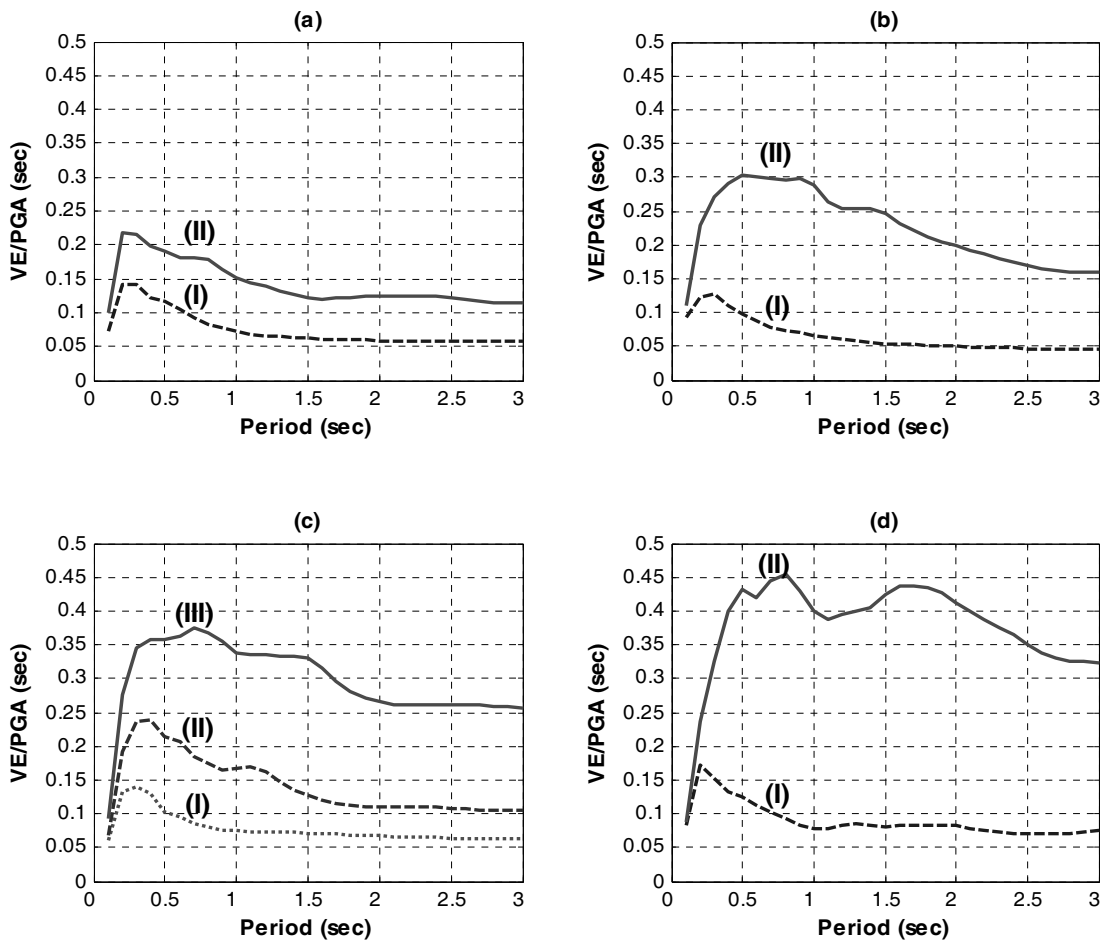


**Fig.6** Mean spectral input energy of the ground motions recorded  
 (a) in ground type 1 (I) for duration  $\leq 6$  sec (II) for duration  $> 6$  sec  
 (b) in ground type 2 (I) for duration  $\leq 8$  sec (II) for duration  $> 8$  sec  
 (c) in ground type 3 (I) for duration  $\leq 7$  sec (II) for  $7 \text{ sec} > \text{duration} \leq 10$  sec (III) for duration  $> 10$  sec  
 (d) in ground type 4 (I) for duration  $\leq 10$  sec (II) for duration  $> 10$  sec

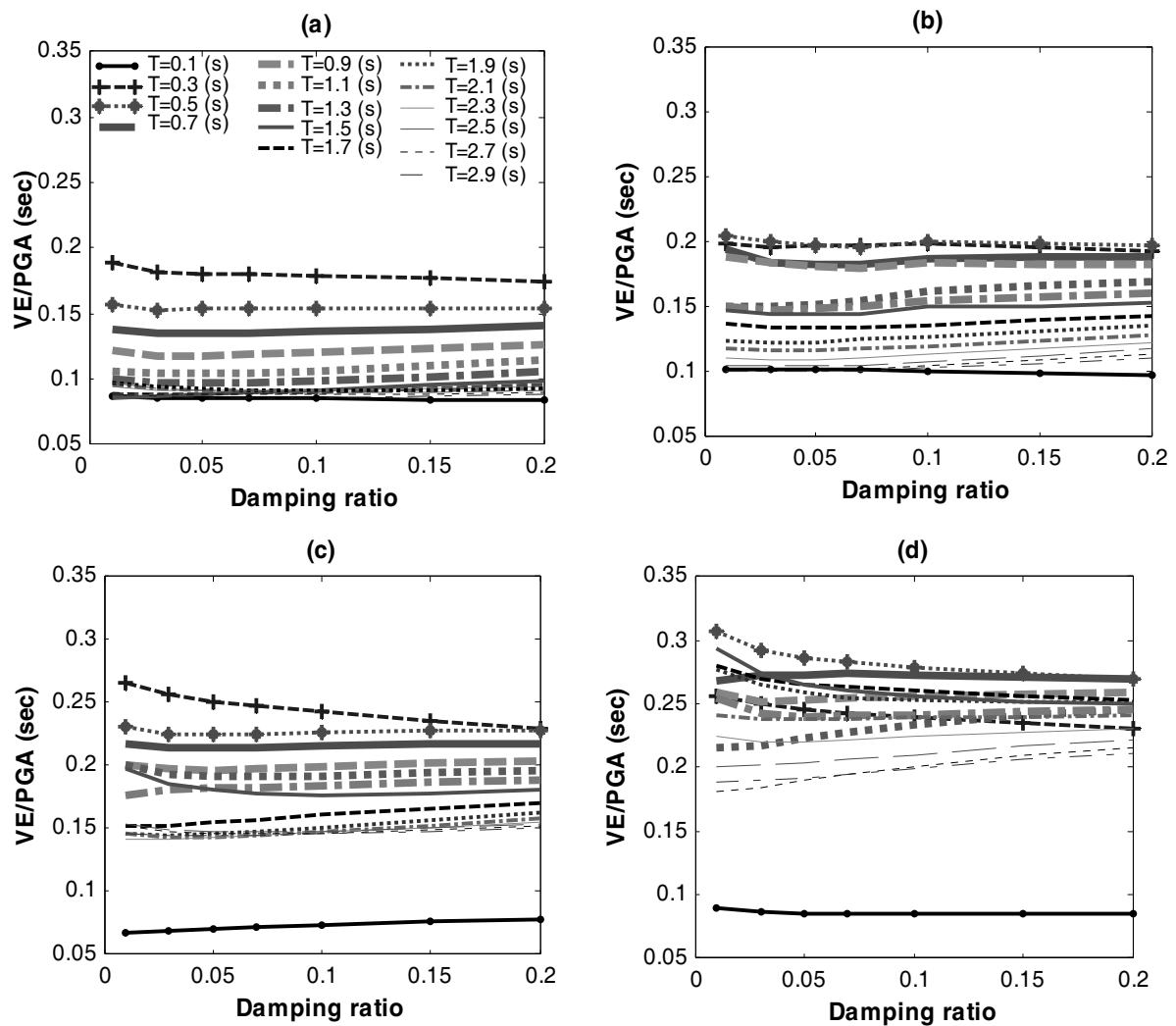


**Fig.7** Spectral input energy versus damping ratio for structures with different natural periods of the ground motions recorded in ground  
 (a) type 1 (b) type 2 (c) type 3 (d) type 4

energy spectra were calculated for different damping ratios using dynamic response analyses and expressed in terms of pseudo-velocity  $V_E$ . Next  $V_E$  was normalized with respect to the absolute peak ground acceleration of the result of two horizontal components ( $PGA$ ). Finally by investigating obtained curves following results were concluded for all of ground types:

**a.** Averagely with an increase in duration, input energy increases considerably, but curve input energy versus duration for each

natural period doesn't necessarily increase.

**b.** With an increase in the amount of damping, input energy decreases for damping ratios smaller than 5% and inverses for damping ratios more than 5%, (in the other words, the amount of input energy in 5% damping ratio is minimum). Of course this variation is not very considerable.

**c.** In all of ground types, input energy in very short natural periods ( $T \leq 0.2s$ ) is almost constant but in longer natural periods, input

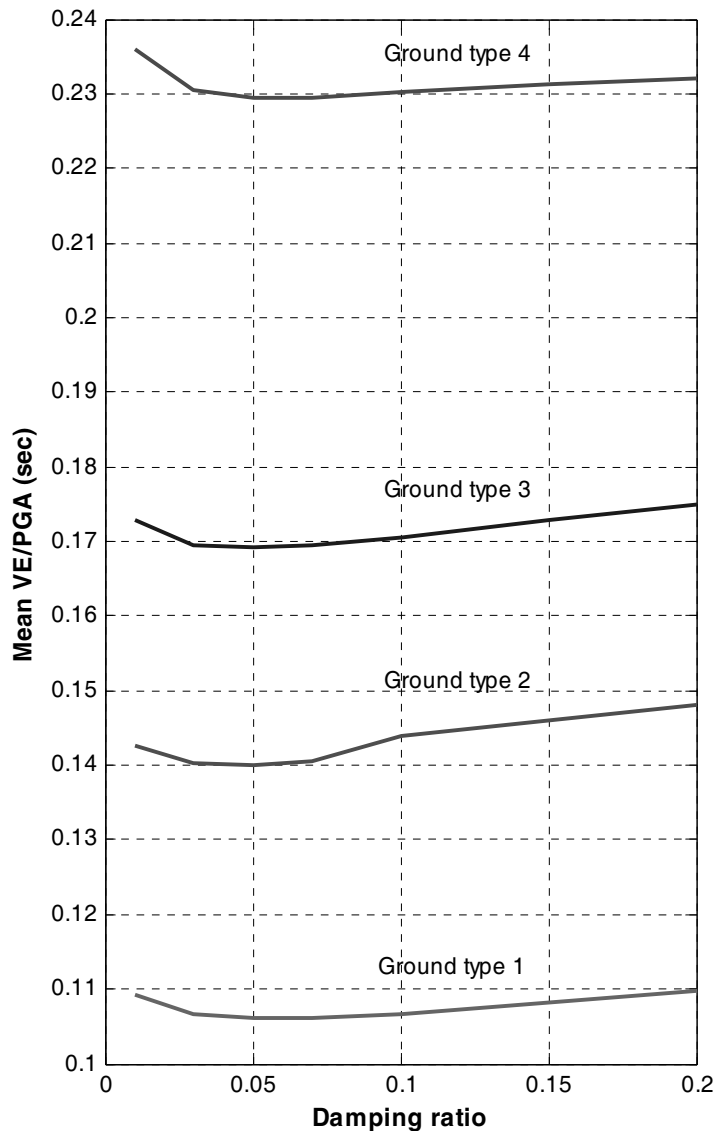


**Fig.8** Mean spectral input energy versus damping ratio for structures with different natural periods of the ground motions recorded in four ground types

energy increases with decreasing in soil stiffness where earthquake records are registered.

## 7. References

- [1] Akbas, B., Shen, J. and Hao, H. [2001] "Energy approach in performance-based seismic design of steel moment resisting frames for basic safety objective", *The Structural Design of Tall Buildings*, 10(3), 193-217.
- [2] Benavent-Climent, A., Pujades, L.G. and Lopez-Almansa, F. [2002] "Design energy input spectra for moderate-seismicity regions", *Earthquake Engineering and Structural Dynamics*, 31, 1151-1172.
- [3] Decanini, L.D. and Mollaioli, F. [2001]

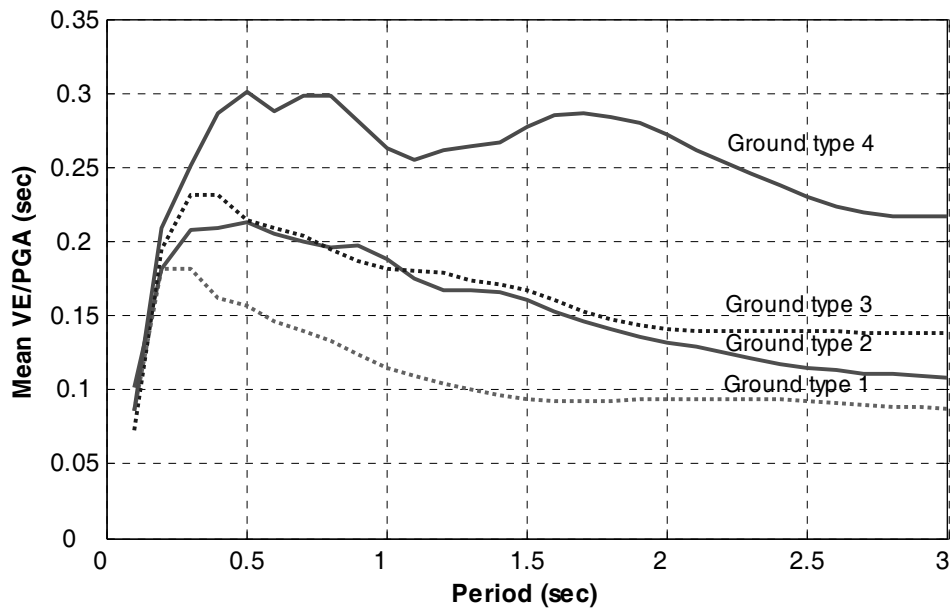


**Fig.9** Mean spectral input energy of ground motions recorded in four ground types for structures with different natural periods

- “An energy-based methodology for the assessment of seismic demand”, *Earthquake Engineering and Structural Dynamics*, 21, 113-137.
- [4] Decanini, L.D. and Mollaioli, F. [1998] “Elastic earthquake input energy spectra”, *Earthquake Engineering and Structural Dynamics*, 27, 1503-1522.
- [5] Leelataviwat, S., Goel, S. and Stojadinovic, B. [1999], “Toward performance-based seismic design of structures”, *Earthquake Spectra*, 15(3), 435-461.
- [6] Manfredi, G. [2001], “Evaluation of seismic energy demand”, *Earthquake Engineering and Structural Dynamics*, 30(4), 485-499.
- [7] Ordaz, M., Huerta, B. and Reinoso, E. [2003], “Exact computation of input energy spectra from Fourier amplitude spectra”, *Earthquake Engineering and Structural Dynamics*, 32, 597-605.
- [8] Trifunac, M.D., Hao, T.Y. and Todorovska, M.I. [2001], “Energy of earthquake response as a design tool”, *Proceedings of the 13th Mexican Conference on Earthquake Engineering*, Guadalajara, Mexico.
- [9] Uang, C.M. and Bertero, V.V. [1990], “Evaluation of seismic energy in structures”, *Earthquake Engineering and Structural Dynamics*, 19, 77-90.
- [10] Akiyama, H. [1999] “Earthquake-resistant design method for buildings based on energy balance”, *Gihodo Shuppan*, Tokyo, 25-26.
- [11] Zahrah, T.F. and Hall, W.J. [1984], “Earthquake energy absorption in SDOF structures”, *Journal of Structural Engineering*, ASCE, 110(8), 1757-1772.
- [12] McKeivitt, W.E., Anderson, D.L. and Cherry, S. [1980], “Hysteretic energy spectra in seismic design”, *Proceedings*

of the 7th World Conference on Earthquake Engineering, 7, 487-494.

- [13] Akiyama, H. [1985] "Earthquake-resistant limit-state design for buildings", University of Tokyo Press, Tokyo.
- [14] Nakashima, M., Saburi, K. and Tsuji, B. [1996], "Energy input and dissipation behavior of structures with hysteretic dampers", Earthquake Engineering and Structural Dynamics, 19(1), 77-90.
- [15] Bruneau, M. and Wang, N. [1996] "Normalized energy-based methods to predict the seismic ductile response of SDOF structures", Engineering Structures, 18, 13-28.
- [16] Rahnama, M. and Manuel, L. [1996], "The effect of strong motion duration on seismic demands", Proceedings of the 11th World Conference on Earthquake Engineering, Mexico, Paper No. 924.
- [17] Khashaei, P., Mohraz, B., Sadek, F., Lew, H.S. and Gross, J.L. [2003], "Distribution of earthquake input energy in structures", Report No. NISTIR 6903, Building and Fire Research Laboratory, National Institute of Standards and Technology, Gaithersburg, MD 20899.
- [18] Trifunac, M.D. and Brady, A.G. [1975], "A study of the duration of strong earthquake ground motion", Bulletin of the Seismological Society of America, 65, 581-626.
- [19] Ahmadizadeh, M. and Shakib, H. [2004] "On the December 26, 2003, southeastern Iran earthquake in Bam region", Engineering Structures, 26, 1055-1070.
- [20] Mahdavian, A. [2000], "Design response spectra for large dams in Iran", China, International Commission of Large Dams (ICOLD).
- [21] Mirzaei, H. and Farzanegan, E. [1999], "Specifications of the Iranian accelerograph network stations", BHRC Publication No. 266, Tehran, Iran, Building & Housing Research Center.
- [22] Zare, M., Bard, P.Y. and Ghafory-Ashtiany, M. [1999a], "The Iranian accelerometric data bank: a revision and data correction", Journal of Seismology and Earthquake Engineering (Tehran, Iran), 1(1), 1-22.
- [23] Zare, M., Bard, P.Y. and Ghafory-Ashtiany, M. [1999b], "Site characterization for the Iranian strong motion network", Soil Dynamics and Earthquake Engineering, 18(2), 101-23.
- [24] Iranian Code of Practice for Seismic Resistance Design of Buildings, Standard No. 2800, 3rd Edition [2005], Building and Housing Research Center, Tehran, Iran.
- [25] Ghodrati Amiri, G. and Manouchehri Dana, F.M. [2005], "Introduction of the most suitable parameter for selection of critical earthquake", Computer and Structures, 83, 613-626.
- [26] Ghodrati Amiri, G., Motamed, R. and Rabet Es-Haghi, H. [2003], "Seismic hazard assessment of metropolitan Tehran, Iran", Journal of Earthquake Engineering; 7(3), 347-372.